J Mater Sci (2010) 45:5553–5557
DOI 10.1007/s10853-010-4616-z

Effects of V and Nb on static recrystallisation of austenite and precipitate size in microalloyed steels

S. F. Medina · M. Gómez · P. P. Gómez

Received: 16 February 2010 / Accepted: 11 May 2010 / Published online: 20 May 2010

Abstract Recrystallisation and precipitation in two microalloyed steels, one with Nb and the other with V, have been studied. The Nb-steel displayed two plateaus on the curves of recrystallised fraction against time. The difference between activation energies allow to predict the efficiency of different precipitates to strengthen the austenite during hot rolling. RPTT diagrams showed the interaction between both phenomena. It is found that NbCN particles nucleate and grow faster than VCN, but the latter are smaller.

Introduction

The type and amount of microalloying elements have an important effect on the shape and the nature of precipitates. Fine VN, VC and Nb(C,N) precipitates inhibit static recrystallisation of austenite, which leads to austenite strengthening during last hot rolling passes. At equal level of microalloying, the precipitates are soluble in austenite as follows [1, 2]: Nb(C,N) < VN < VC.

Nitrides and carbides of typical microalloying elements (Nb,V) have an f.c.c. crystallographic structure. These compounds, especially in the case of the smallest particles, frequently form precipitates which are semi-coherent with the (f.c.c.) austenitic matrix. Their lattice parameter is slightly higher than that of the austenite [3].

The size and volume fraction of precipitates play an important role on pinning forces, both for austenite grain growth control at any reheating temperature and for inhibition of austenite static recrystallisation during hot rolling. The latter causes a strengthening of austenite and an increase in dislocation density that in turn multiplies the number of potential nucleation sites for ferrite [4–8].

In this work the recrystallisation of two microalloyed steels with V and Nb is studied from the point of view of its inhibition due to strain-induced precipitation. Precipitate size is determined in both steels by means of TEM observations, which lets to establish important differences between both types of precipitates.

Materials and experimental procedure

Chemical compositions of steels used are shown in Table 1. The specimens for torsion testing had a gauge length of 50 mm and a diameter of 6 mm. The austenitisation temperature was set to be higher than the solubility temperature of precipitates, thus assuring that the precipitates would be completely dissolved in the austenite. The mean austenite grain size corresponding to the austenitisation conditions was determined for each steel by applying ASTM E-112 standard (Table 2). The coarser grain size of steel A is caused by the lower solubility temperature of V precipitates (T_s), which implies a faster austenite grain growth rate [1].

After austenitisation at 1200 °C during 10 min, the specimens were rapidly cooled to the deformation temperature in order to prevent precipitation prior to deformation. The deformation temperatures were between 1100

S. F. Medina (✉) · M. Gómez · P. P. Gómez
National Centre for Metallurgical Research (CENIM-CSIC),
Av. Gregorio del Amo 8, 28040 Madrid, Spain
e-mail: smedina@cenim.csic.es

M. Gómez
e-mail: mgomez@cenim.csic.es

P. P. Gómez
e-mail: pedropg@cenim.csic.es

Table 1 Chemical composition of steel used (% mass × $10^{3)}$

Steel	C	Mn	Si	Al	V	Nb	Ti	N
A	94	1475	329	21	92	–	–	6.5
B	90	1505	313	17	–	34	–	4.0

Table 2 Austenite grain size ($\bar{d}$)

Steel	Reheating conditions	$\bar{d}$ (μm)
A	1200 °C × 10 min	151
B	1200 °C × 10 min	107

and 800 °C, and the recrystallised fraction (X_a) was determined for several holding times after deformation. The applied strain was 0.35, which was insufficient to promote dynamic recrystallisation [9]. The double deformation technique was used to calculate X_a, in particular applying the method known as "back extrapolation" [10].

Results and discussion

It is very well-known that static recrystallisation is a nucleation and growth process, as happens with the precipitation of VN or Nb(C,N) particles and many other phenomena such as the precipitation of Cr nitrides and carbides [11] or the precipitation of intermetallic phases in a metallic matrix [12–14].

The shape of the curves of recrystallised fraction against time for the V and Nb-microalloyed steels presented one and two plateaus, respectively, when the test temperatures were below those where the particles have precipitated. Figure 1 shows the recrystallised fraction for steel A at several temperatures, with a plateau appearing on the curves corresponding to 900 and 850 °C. The start and

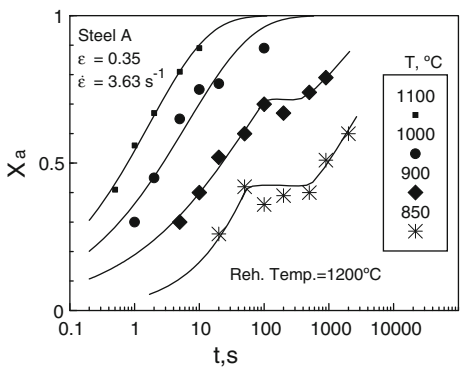

Fig. 1 Recrystallised fraction (X_a) vs. time (t) for steel A

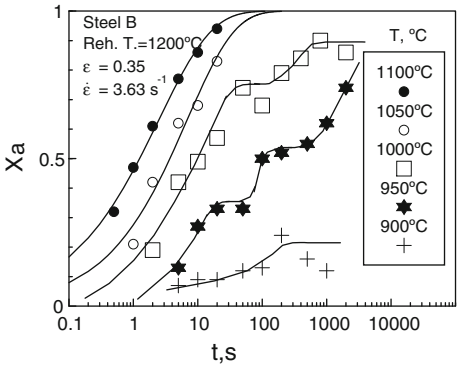

Fig. 2 Recrystallised fraction (X_a) vs. time (t) for steel B

finish of the plateau are identified approximately with the start and finish of the induced precipitation [15].

Figure 2 presents the recrystallised fraction for steel B showing two plateaus in the curves plotted at 1000 and 950 °C. This phenomenon is a result of the appearance of two types of carbonitrides which start to form at practically the same temperature, but the second precipitation is promoted by the first when the nitrogen or carbon content is reduced. It should also be said that double precipitation only appears when the solubility temperatures for Nb nitrides and carbides take very similar values [16–18].

Figures showing the recrystallised fraction versus time were used to deduce the temperature and times corresponding to different recrystallised fractions. The points that define the start and the end of the plateau were taken to plot the induced precipitation start (P_s) and finish (P_f) curves, respectively. In this way recrystallisation–precipitation–time–temperature (RPTT) diagrams for the studied steels were drawn. The recrystallised fraction does not vary between the precipitation start (P_s) and finish (P_f) curves and is represented by a horizontal line. Once the P_f curve is reached, the lines of each recrystallised fraction descend again (Figs. 3, 4). In the case of Fig. 4, corresponding to the steel B, two P_s and two P_f curves have been drawn, as a consequence of the double precipitation.

The values of the minimum incubation time for precipitates (t_N) and the curve nose temperature (T_N) are shown in Table 3. Nb(C,N) particles nucleate earlier and grow faster than VN particles.

With regard to the recrystallisation–precipitation interaction, it is seen that the recrystallised fraction is approximately 50% at the nose of the P_s curve, i.e., at the place where the incubation time of the precipitates (t_N) takes the shortest value. When the fraction of recrystallised volume is less than 20%, nucleation of the precipitates needs longer time to take place.

The static recrystallisation kinetics of austenite when the microalloying elements (V, Nb) are in solution can be described by an Avrami equation in the following way [9]:

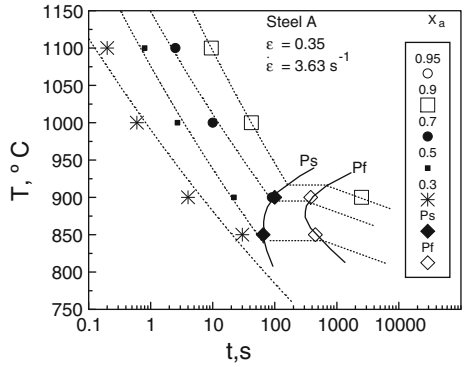

Fig. 3 RPTT diagram. Steel A

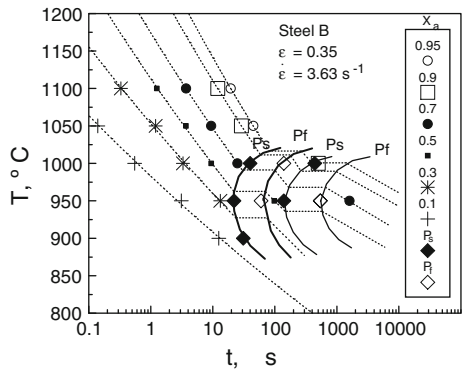

Fig. 4 RPTT diagram. Steel B

Table 3 T_N and t_N of the P_s curve nose

Steel	ε	t_N (s)	T_N (°C)
A	0.35	65	875
B	0.35	23	950

$$X_a = 1 - exp\left[-0.693\left(\frac{t}{t_{0.5}}\right)^n\right] \quad (1)$$

where X_a is the fraction of the recrystallised volume and $t_{0.5}$ is the time corresponding to 50% recrystallisation, which depends practically on all the variables that intervene in hot deformation and whose most general expression can be defined by the equation:

$$t_{0.5} = A\varepsilon^p\dot{\varepsilon}^q D^s \exp\frac{Q_x}{RT} \quad (2)$$

where ε is the strain, $\dot{\varepsilon}$ the strain rate, D the grain size, Q_x the activation energy, T the absolute temperature, $R = 8.3145$ J mol^{-1} K^{-1}, and p, q, s, and A are parameters. While p and q are negative values, s is positive.

On the other hand, the activation energy (Q_x) for the static recrystallisation of austenite in the presence of precipitates may be expressed as the sum of two terms [17]:

$$Q_x = Q + \Delta Q \quad (3)$$

where Q represents the activation energy in the absence of precipitates and ΔQ represents the increase due to the presence of the precipitates. In accordance with Eq. 2, Fig. 5 displays the parameter $t_{0.5}$ against the inverse of the absolute temperature for steel A. The line of ln $t_{0.5}$ against $1/T$ shows a discontinuity just when the temperature reaches the curve P_s. The value of the activation energy changes from one stage to another. After precipitation the activation energy increases significantly, which is obviously translated into greater difficulty for the austenite to recrystallise. The figure allows the values of Q and $Q + \Delta Q$ to be calculated. The comparison of the values shown in Table 4 demonstrates that the contribution of precipitates to the increment in activation energy (ΔQ) is higher for VN than for Nb(C,N) due to the finer size of precipitates and the higher precipitate volume for VN. When V and Nb are in solution, i.e., in the absence of precipitates, the value of Q is higher in steel B because, according to established models of recrystallisation kinetics [15], Nb exerts a stronger solute drag effect than V.

In order to know the type and size of the precipitates, a study was carried out using transmission electron microscopy (TEM) techniques on carbon extraction replicas (Fig. 6). The specimens were heated at reheating temperature and then the temperature was lowered to that corresponding to the nose temperature in RPTT diagram with a holding time up to the P_f curve, which coincides with the

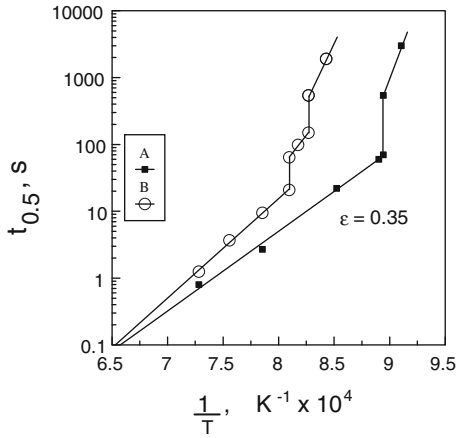

Fig. 5 Plot of $t_{0.5}$ against the reciprocal of the absolute temperature

Table 4 Activation energy for static recrystallisation

Steel	Q (kJ)	Q + ΔQ (kJ)	ΔQ (kJ)
A	215	695	480
B	295	600	305

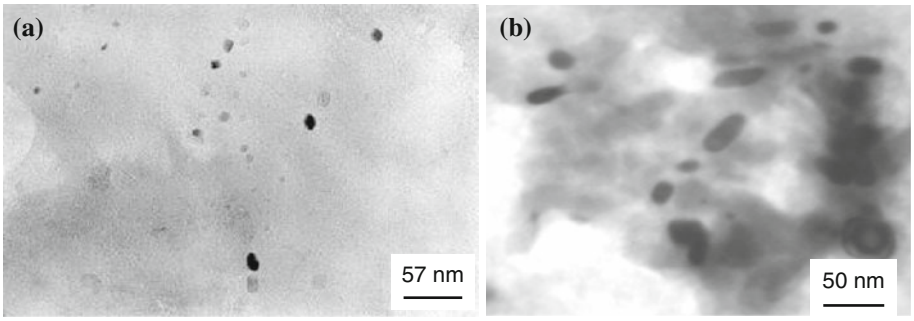

Fig. 6 TEM image of precipitates. **a** VN—Steel A; **b** Nb(C,N)—Steel B

Table 5 Mean size of precipitates

Steel	Particle type	Mean size (nm)
A	VN	10.5
B	Nb(C,N)	22

end of the plateau on corresponding curve of recrystallised fraction vs. time. The values found for the mean size are shown in Table 5. Mean size of VN in steel A was equal to 10.5 nm and mean size of Nb(C,N) in steel B was equal to 22 nm. The values found for Nb(C,N) precipitates are similar to those found by other authors [19, 20].

On the other hand, the particle diameter at any temperature can be expressed as [21, 22]:

$$\Delta d^2 = \alpha^2 D_0 \exp\left(-\frac{Q_d}{RT}\right)\Delta t \tag{4}$$

where $\Delta d^2 = d^2 - d_0^2$ and $\Delta t = t - t_0$. Here, d_0 is the particle diameter at time t_0, α is the growth coefficient and $D_0 \exp\left(-\frac{Q_d}{RT}\right)$ is the diffusion coefficient (D) of V and Nb in austenite, being the expressions for both [21, 23]:

$$D_V = 3.05 \times 10^{-4} \exp\left(-\frac{239300}{RT}\right) \tag{5}$$

$$D_{Nb} = 1.49 \times 10^{-4} \exp\left(-\frac{234700}{RT}\right) \tag{6}$$

where activation energy for diffusion (Q_d) is expressed in J. The values of D_V and D_{Nb} are expressed in m^2/s and were calculated at the temperature corresponding to the nose of the P_s curve (Table 6).

Coefficient D is higher for Nb than for V. Besides, temperature T_N is higher for steel B compared to steel A and the same is true for T_s temperature. This explains why Nb(C,N) precipitates are coarser than VN precipitates.

Table 6 Values of D_V and D_{Nb} at T_N temperatures

Steel	T_N (K)	D (m^2/s)
A	1148	3.9471×10^{-15}
B	1223	1.4103×10^{-14}

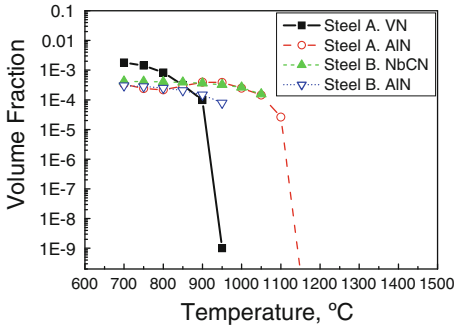

Fig. 7 Precipitated volume fraction of particles against temperature

For the calculation of pinning forces consideration was made of the expression of Zener [24], which is proportional to reciprocal of precipitate size:

$$F_p = \frac{3f\gamma}{2r} \tag{7}$$

where γ is the interfacial energy per grain boundary unit area (0.8 J/m^2 in austenite), f is the precipitated volume fraction and r is the mean radius of precipitates. The values of precipitated volume fraction (f) for VN and Nb(C,N) particles were calculated in accordance with Hillert's model [25] and the results are shown in Fig. 7, where precipitated volume fractions for AlN particles are also plotted. The volume fraction of precipitates is somewhat higher for VN than for Nb(C,N). The latter, together with the finer mean particle size in steel A helps to explain the higher value of ΔQ in steel A.

Conclusions

The main conclusions are as follows: larger diffusion coefficient of Nb compared to V, together with the higher precipitation temperature of Nb(C,N) serve to explain the coarser size of NbCN particles compared to VN. On the other hand, steel A presents an increase of activation energy due to precipitation (ΔQ) higher than steel B because of the smaller mean size and the higher volume

fraction of VN precipitates in steel A compared to Nb(C,N) precipitates in steel B.

References

1. Turkdogan ET (1989) Iron Steelmaker 3:61
2. Narita K (1975) Trans Iron Steel Inst Jpn 15:145
3. Gladman T (1997) The physical metallurgy of microalloyed steels. The Institute of Materials, London
4. Vega MI, Medina SF, Quispe A, Gómez M, Gómez PP (2006) Mater Sci Eng A 423:253
5. Gao N, Baker TN (1998) ISIJ Int 38:744
6. Medina SF, Gómez M, Rodríguez E, Rancel L (2008) ISIJ Int 48:1263
7. Quispe A, Medina SF, Valles P (1997) ISIJ Int 37:783
8. Cabibbo M, Fabrizi A, Merlin M (2008) J Mater Sci 43:6857. doi:10.1007/s10853-008-3000-8
9. Sellars CM (1980) Hot working and forming processes. Metals Society, London
10. Perttula JS, Karjalainen LP (1998) Mater Sci Technol 14:626
11. Calliari I, Brunelli K, Zanellato M, Ramous E, Bertelli R (2009) J Mater Sci 44:3764. doi:10.1007/s10853-009-3505-9
12. Pardal JM, Tavares SSM, Fonseca MPC, Souza JÁ, Loureiro A, Moura EP (2010) J Mater Sci 45:616. doi:10.1007/s10853-009-3935-4
13. Kamada Y, Takahashi S, Kikuchi H, Kobayashi S, Ara K, Echigoya J, Tozawa Y, Watanabe K (2009) J Mater Sci 44:949. doi:10.1007/s10853-008-3182-0
14. Vasconcelos I, Tavares S, Reis F, Abreu H (2009) J Mater Sci 44:293. doi:10.1007/s10853-008-3064-5
15. Medina SF, Quispe A (2001) ISIJ Int 41:774
16. Medina SF, Quispe A, Gómez M (2001) Mater Sci Technol 17:536
17. Medina SF, Quispe A, Gómez M (2003) Mater Sci Technol 19:99
18. Gómez M, Medina SF, Valles P, Quispe A (2005) Mater Sci Forum 480–481:489
19. Wang HR, Wang H (2009) J Mater Sci 44:591. doi:10.1007/s10853-008-3069-0
20. Lu SP, Wei ST, Li DZ, Li Y (2010) J Mater Sci 45:2390. doi:10.1007/s10853-010-4205-1
21. Park SH, Yue S, Jonas JJ (1992) Metall Trans A 23:1641
22. Okaguchi S, Hashimoto T (1992) ISIJ Int 32:283
23. Oikawa H (1982) Tetsu-to-Hagane 68:1489
24. Smith CS (1948) Trans AIME 175:15
25. Hillert M, Staffanson LI (1970) Acta Chem Scand 24:3618